Microvoids in Polyacrylonitrile Fibers: A Small-Angle X-ray Scattering Study

Andreas F. Thünemann*

Max Planck Institute of Colloids & Interfaces, Am Mühlenberg, 14476 Golm, Federal Republic of Germany

W. Ruland

Fachbereich Chemie und Zentrum für Materialwissenschaften, Philipps-Universität Marburg, Federal Republic of Germany

Received August 23, 1999; Revised Manuscript Received November 29, 1999

ABSTRACT: The formation of microvoids in polyacrylonitrile (PAN) fibers was studied as a function of temperature by synchrotron small-angle X-ray scattering (SAXS). The microvoids show preferred orientation and have elongated shapes with lengths in the range of 30 to 100 nm and diameters in the range of 0.5 to 3.0 nm. In the pristine fibers, the microvoid content is of the order of one volume percent, the length is 30−40 nm, and the diameter 2−3 nm. It was found that varying numbers of additional microvoids are formed in a temperature range of 190 °C to 470 °C. In the final stage, the content of microvoids is of the order of 10−20 volume percent, and their lengths and diameters are 40 and 0.5 nm, respectively. The formation of the microvoids is correlated with the cyclization and aromatization reactions of the fibers, which are important steps in the formation of the carbon fiber structure. A detailed SAXS evaluation procedure was used for the quantitative description of orientation, length, diameter, and relative volume of microvoids. The procedure may be of interest for the characterization of microvoid systems in other types of fibers.

1 Introduction

Microvoid systems with preferred orientation are known to be present in carbon fibers[1−3] as well as in PPTA fibers.[5−7] These microvoids are the result of the imperfect packing of the structural units (ribbons of carbon layers in the case of carbon fibers, rigid chain molecules in the case of PPTA) and play an important role in the assessment of mechanical properties, notably the compressive strength. It was shown earlier that a heat treatment of PAN-fibers at 300 °C produces elongated microvoids with lengths in a range of 30 to 46 nm.[8] The main axes of these microvoids are oriented in the direction of the fiber axis. To our knowledge, no systematic investigation has been conducted on the formation of microvoids in the early stages of carbon fiber formation. The present work was carried out in connection with SAXS studies on the mesophase formation occurring during the cyclization and aromatization process, which is the subject of a separate paper.[9] Mesophase formation results in the appearance and disappearance of lamellar systems as a function of heat treatment temperature. The structural inhomogeneities produced by this process lead to the formation of microvoids, which was studied by detailed synchrotron SAXS during the heat treatment of the fibers, and the correlation between microvoid formation and the cyclization and aromatization process was investigated.

2 Theoretical Section

In this section, we shall describe a method of evaluation which offers an optimum of information for a study of a series of 2D SAXS distributions.

We consider a dilute system of elongated microvoids that are oriented with their long axes in the direction of the fiber axis. The values of interest are the length of the microvoids L, the diameter D, and a parameter defining the preferred orientation. To simplify the calculations, we assume a cylindrical shape of the microvoids. In this case, the intensity I_v of a single microvoid is given by

$$I_v(\mathbf{s}) = I_v(s_{12},s_3) = \rho_m^2 |\Phi_D|^2(s_{12}) |\Phi_L|^2(s_3)$$

where ρ_m is the electron density of the matrix in which the microvoids are embedded, $\Phi_D(s_{12})$ is the 2D Fourier transform of the shape function of the cross-section, and $\Phi_L(s_3)$ is the 1D Fourier transform of the shape function of the length. s_{12} and s_3 are the components of the reciprocal space vector $\mathbf{s}$ in the directions perpendicular and parallel to the principal axis of the microvoid, respectively. Alternatively, we can write

$$I_v(\mathbf{s}) = I_v(s, \phi) = \rho_m^2 |\Phi_D|^2 (s \sin \phi) |\Phi_L|^2 (s \cos \phi)$$

where $s = |\mathbf{s}| = (2 \sin \theta)/\lambda$, ϕ is the polar angle, θ is the Bragg angle, and λ is the wavelength. The integral widths of $|\Phi_D|^2$ and $|\Phi_L|^2$ are $1/D$ and $1/L$, respectively. If $L \gg D$, the intensity distribution I_v is represented in reciprocal space by a flat disk extending in the plain perpendicular to s_3 (see Figure 1, upper part).

The intensity distribution of an dilute system of microvoids with uniaxial preferred orientation is given by[10]

$$I(s, \phi) = n\rho_m^2 \int_0^{\pi/2} I_v(s, \phi') F(\phi, \phi') \sin \phi' \, d\phi'$$

where n is the number of microvoids. $F(\phi,\phi')$ is the orientation distribution ("pole figure") as a function of ϕ for the direction ϕ' in a system with simple fiber symmetry

$$F(\phi, \phi') \propto \int_0^{\pi} g_{ax}(\beta) \, d\eta$$

* Corresponding author. E-mail: andreas@mpikg-golm.mpg.de.

10.1021/ma991427x CCC: $19.00
Published on Web 02/10/2000

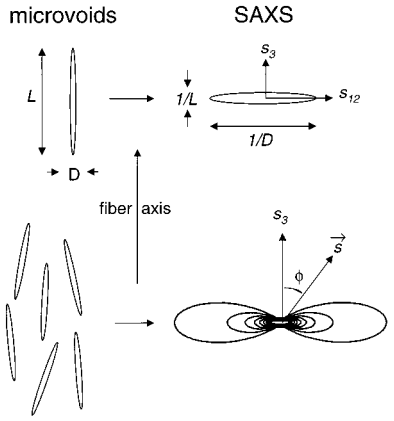

Figure 1. Schematic representation of the scattering intensity of an individual microvoid (upper part) and of a dilute system of microvoids with preferred orientation (lower part).

where

$$\cos\beta = \cos\phi\cos\phi' + \sin\phi\sin\phi'\cos\eta$$

and $g_{ax}(\beta)$ is the orientation distribution of the long axes of the microvoids. Accordingly, $g_{ax}(\phi) \propto F(\phi,0)$ and the corresponding equatorial distribution $g_{eq}(\phi) \propto F(\phi,\pi/2)$.

Qualitatively, $I(s,\phi)$ is represented in reciprocal space by a fan-shaped distribution in the 2D section containing the fiber axis, as already discussed in an earlier paper.[1] Such a distribution is shown schematically in Figure 1, lower part.

If $L \gg D$, and $g_{eq}(\phi)$ is a relatively narrow distribution centered on $\phi = \pi/2$, we can use the approximations

$$F(\phi, \pi/2 - \Delta\phi') \propto g_{eq}(\phi - \Delta\phi') + g_{eq}(\phi + \Delta\phi')$$

and

$$I_v(s, \pi/2 - \Delta\phi') = \rho_m^2 |\Phi_D|^2 (s\cos\Delta\phi') |\Phi_L|^2 (s\sin\Delta\phi')$$

Furthermore, since $\Delta\phi'$ is considered to be small, we put $\cos\Delta\phi' \simeq 1$ and $\sin\Delta\phi' \simeq \Delta\phi'$, which results in

$$I_v(s, \pi/2 - \Delta\phi') \simeq \rho_m^2 |\Phi_D|^2 (s) |\Phi_L|^2 (s\,\Delta\phi')$$

Taking into account the symmetry of $F(\phi,\pi/2 - \Delta\phi')$ and $g_{eq}(\phi)$, this leads to

$$I(s, \phi) = n\rho_m^2 |\Phi_D|^2(s) \int |\Phi_L|^2 (s\,\Delta\phi')\, g_{eq}(\phi - \Delta\phi')\, d\Delta\phi'$$

which we can rewrite as

$$I(s, \phi) = n\rho_m^2 |\Phi_D|^2(s)\, [|\Phi_L|^2 (s\,\phi) *_\phi g_{eq}(\phi)] \qquad (1)$$

where $*_\phi$ stands for a convolution in ϕ. Equation 1 represents the fan-shaped intensity distribution (see Figure 1) discussed above.

For the evaluation, we choose two functions, first the tangential width of the equatorial distribution $B_{\pi/2}(s)$

$$B_{\pi/2}(s) = \frac{1}{I(s, \pi/2)} \int I(s, \phi)\, d\phi$$

$$= \frac{\int [|\Phi_L|^2 (s\,\phi) *_\phi g_{eq}(\phi)]\, d\phi}{[|\Phi_L|^2 (s\,\phi) *_\phi g_{eq}(\phi)]\, (\pi/2)}$$

and, second, the scattering on the equator

$$I(s, \pi/2) = n\rho_m^2 |\Phi_D|^2(s) \frac{1}{B_{\pi/2}(s)} [\int |\Phi_L|^2 (s\,\phi)\, d\phi] \times [\int g_{eq}(\phi)\, d\phi]$$

The latter expression can be simplified to

$$I(s, \pi/2) \propto n\rho_m^2 \frac{L}{s\, B_{\pi/2}(s)} |\Phi_D|^2(s)$$

since

$$\int |\Phi_L|^2 (s\,\phi)\, d\phi = \frac{1}{s} \int |\Phi_L|^2 (s_3)\, ds_3 = \frac{L}{s}$$

and the integral over g_{eq} is considered constant.

The function $B_{\pi/2}(s)$ is the integral width of the convolution in ϕ of $|\Phi_L|^2(s\,\phi)$ and $g_{eq}(\phi)$. If $|\Phi_L|^2$ and g_{eq} can be approximated by Gaussian distributions, we obtain the relationship

$$B_{\pi/2}^2(s) = 1/(sL)^2 + B_{eq}^2 \qquad (2)$$

where $1/(sL)$ and B_{eq} are the integral widths of $|\Phi_L|^2(s\,\phi)$ and $g_{eq}(\phi)$, respectively. For other types of distributions, different relationships have to be used (see e.g., ref 11). It should be noted that a Gaussian approximation for a narrow g_{eq}, for example, $g_{eq}(\phi) \propto |\sin^\nu \phi|$ for $\nu \gg 1$, implies B_{eq} to be equal to the width of the axial orientation distribution B_{ax}.

With this approximation, we finally obtain

$$I(s, \pi/2) \propto n\rho_m^2 \frac{L^2}{\sqrt{1 + (sLB_{eq})^2}} |\Phi_D|^2(s) \qquad (3)$$

For the evaluation, we first compute $B_{\pi/2}(s)$ from plots of $I(s,\phi)$ at constant s values, which results in the determination of L and B_{eq}, for example, from plots of $s^2\, B_{\pi/2}^2(s)$ versus s^2 if these are linear. Inserting the values in eq 3, we determine $|\Phi_D|^2(s)$, and by a suitable curve fitting we obtain the relative number of microvoids and a parameter related to the cross-section of the microvoids. Since we expect a relatively large distribution of diameters, an expression of the form

$$|\Phi_D|^2(s) \propto \frac{l_p^4}{[1 + (2\pi l_p s)^2]^{3/2}} \qquad (4)$$

appears to be an acceptable approximation for the intensity distribution in the cross-section of the microvoids. It is related to the Fourier Bessel transform of a 2D correlation function of the type

$$\gamma(r) = \exp\left(-\frac{r}{l_p}\right)$$

where l_p is the average chord-length (Porod length) in the cross-section of the microvoids. The corresponding chord-length distribution g,

$$g(r) = \frac{1}{l_p} \exp\left(-\frac{r}{l_p}\right)$$

is nonzero at $r = 0$. This means that the contour of the cross-sections is assumed to be angular, comparable to

those observed in PAN-based carbon fibers.[3] It should be noted that the 2D correlation function is considered to be an approximation for the cross-section of single microvoids and should not be confused with the 3D correlation function for random scatterer used by Debye et al.[4]

Provided that ρ_m and the irradiated mass of the sample do not change significantly during the measurements, the fitting procedure results, in addition to l_p, in the determination of the relative number n of microvoids for a given sample. This parameter can be used to calculate the relative total volume of microvoids $V \propto n\ L\ l_p^2$. It should be noted that the parameters n, B_{eq}, L, and l_p are independent of the volume concentration of voids. For B_{eq} and L, this is true since these parameters are derived from an extrapolation of the tangential width $B_{\pi/2}(s)$ of the equatorial intensity distribution. For n and l_p this is true since the microvoids represent the minority phase and are considered to be randomly spaced in the matrix without contact of the surfaces. Furthermore, the intensity is fitted predominantly at medium and large s values where the scattering of the single microvoids prevails.

3 Experimental Section

The first type of PAN fibers investigated was a PAN homopolymer (<0.7% methyl acrylate) produced by Hoechst (Dolanit). The homopolymer fibers have initial tensile moduli of about 17 GPa, extensions at break of about 8%, and diameters of about 16 μm. The second type was PAN a copolymer fiber produced by Sigri that contains 2 to 6% methyl acrylate and itaconic acid. The copolymer fibers have initial tensil moduli of about 11 GPa, extensions at break of 17%, and diameters of about 14 μm. Temperature-dependent SAXS measurements were performed at DESY in Hamburg at the polymer beamline A2, Germany, using radiation with a wavelength of 0.145 nm. The measurements were repeated four times for the homopolymer and the copolymer fibers. The heating rate was 20 K/min for both samples. The combination of synchrotron radiation and a two-dimensional position-sensitive detector was necessary to follow the kinetics of microvoid formation during the cyclization and the aromatization. 2D intensity distributions were measured in intervals of 20 K in the range from 190 °C to 470 °C. The integral widths of the primary beam, measured on the scale of $s = (2 \sin \theta)/\lambda$, were $B_{12} = 0.03$ nm^{-1} and $B_3 = 0.01$ nm^{-1} in the direction of s_{12} and s_3, respectively.

4 Results and Discussion

In addition to the meridional SAXS due to lamellar mesophases, already treated in a recent paper,[9] the PAN fibers show an equatorial scattering (see Figure 2) which corresponds to that described in the theoretical section. We first compute the function $B_{\pi/2}(s)$ from tangential scans of the 2D scattering distribution. Using eq 2 in the form

$$s^2\ B_{\pi/2}^2(s) = 1/L_{app}^2 + s^2\ B_{eq}^2$$

we observed a linear relationship in a plot of $s^2\ B_{\pi/2}^2(s)$ versus s^2, which proves that the Gaussian approximation is valid. From this plot, we obtain the values of B_{eq} and the apparent length L_{app}. The latter is related to

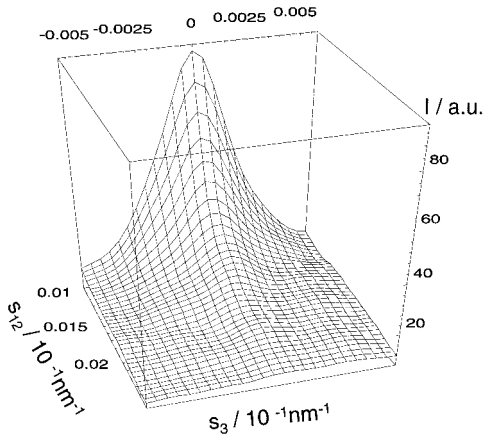

Figure 2. Scattering pattern of PAN homopolymer fibers near the equator at 350 °C.

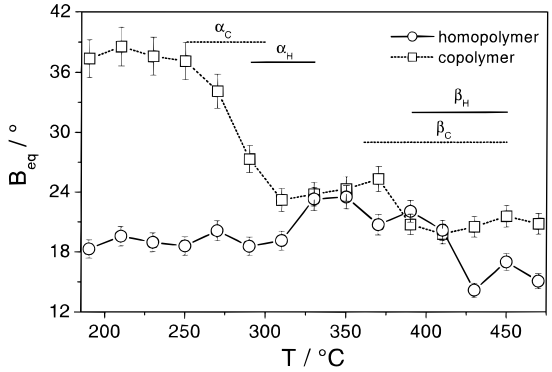

Figure 3. Temperature dependence of the width B_{eq} of the equatorial orientation distribution of the microvoids for homopolymer fibers (circles) and copolymer fibers (squares). The appearance of the α and the β phases is indicated as horizontal lines.

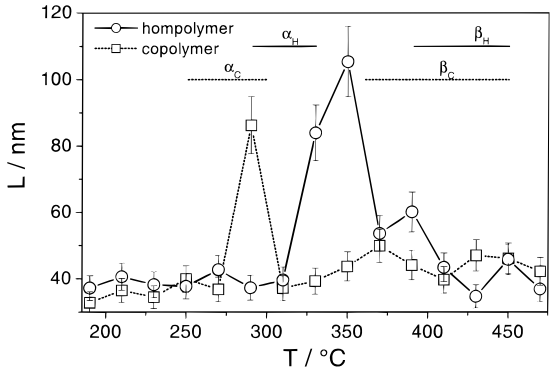

Figure 4. Temperature dependence of the length L of the microvoids for homopolymer fibers (circles) and copolymer fibers (squares). The appearance of the α and the β phases is indicated as horizontal lines.

the true length L by the relationship

$$1/L^2 = 1/L_{app}^2 - B_3^2$$

since the width of the primary beam B_3 in the direction of the fiber axis has to be taken into account ("desmearing") in this calculation. Figures 3 and 4 present the results of the evaluation of B_{eq} and L.

After this, we used eqs 3 and 4 to obtain the parameters l_p and n by fitting theoretical to experimental $I(s,\pi/2)$ curves. The effect of B_3 is taken into account by using L_{app} instead of L in eq 3. Examples of the fit

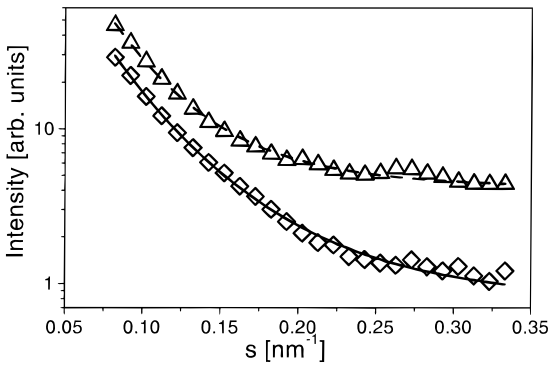

Figure 5. Scattering curves $I(s,\pi/2)$ of the homopolymer and fits according to eqs 3 and 4 at 190 °C (diamonds) and 320 °C (triangles).

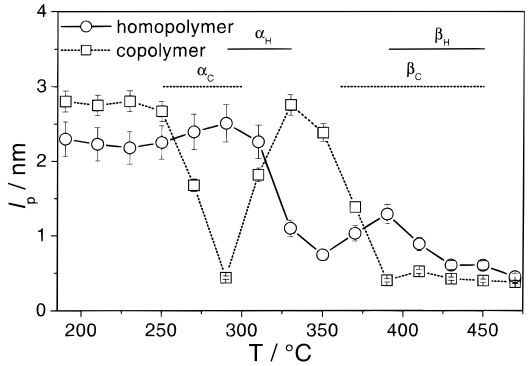

Figure 6. Temperature dependence of the average chord length l_p in the cross-section of the microvoids for homopolymer fibers (circles) and copolymer fibers (squares). The appearance of the α and the β phases is indicated as horizontal lines.

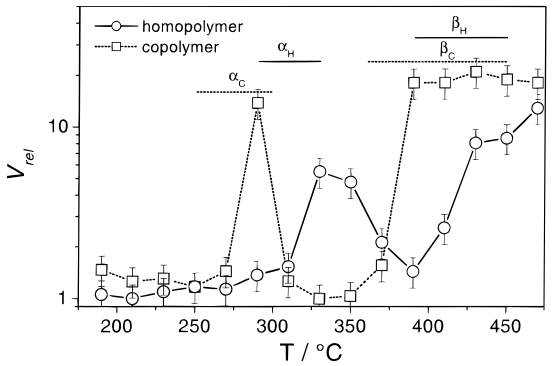

Figure 7. Temperature dependence of the relative total volume V_{rel} of microvoids for homopolymer fibers (circles) and copolymer fibers (squares). The appearance of the α and the β phases is indicated as horizontal lines.

are shown in Figure 5. Since the curves are slowly varying in s, the effect of B_{12} on $I(s,\pi/2)$ can be neglected. Figures 6 and 7 show the results obtained for the parameters l_p and $V_{rel} = V/V_{min}$, where V_{min} is the minimum value of $V = nLl_p^2$ obtained in the homopolymer and the copolymer fibers, respectively.

The preferred orientation of the microvoids as determined by B_{eq} is, at lower temperatures, much higher in the homopolymer fibers than in the copolymer fibers. This is probably due to the difference in the molecular orientation in the pristine fibers. In the temperature range where the α phase starts to disappear, both fibers show about the same value of B_{eq} which, in the case of the copolymer fibers, is much lower than the starting value. The appearance of the β phase is accompanied by a small decrease of B_{eq} for both types of fibers.

The length L of the microvoids shows a maximum (105 nm for homopolymer fibers, 85 nm for copolymer fibers) in the temperature range where the α phase starts to disappear, that is, where the cyclization reaction is nearly completed. Outside of this range, L is about 30−40 nm.

The average chord-length in the cross-section l_p starts with values of 2.3 nm for homopolymer fibers and 2.8 nm for copolymer fibers. In the temperature range where the α phase starts to disappear, l_p drops below 1 nm for both fibers and rises again. The temperatures of the minima of l_p correspond to those of the maxima of L. The appearance of the β phase is accompanied by a steady decrease toward $l_p \simeq 0.5$ nm. It is of interest to note that this value corresponds roughly to that measured for PAN-based carbon fibers with a heat treatment temperature of 1250 °C ($l_p = 0.62$ nm)[3].

The relative total volume of microvoids V_{rel} is very low at lower temperatures. It shows a pronounced maximum in the temperature range where the α phase starts to disappear. The appearance of the β phase is accompanied by a steep increase of V_{rel} for copolymer fibers and a smooth increase for homopolymer fibers. Since PAN-based carbon fibers with a heat treatment temperature of 1250 °C are known to contain a volume fraction of microvoids of about 0.11,[3] the V_{rel} values can be expected to correspond roughly to volume percent values.

To understand the correlation between the formation of microvoids and the structural changes in the fibers, it should be noted that the α phase is a lamellar system composed of pristine chain segments and cyclized chain segments and the β phase is a lamellar system composed of cyclized chain segments and aromatized chain segments.[9] These phases appear and disappear during the heat treatment. Between the α and the β phase, the fiber is completely cyclized, and after the β phase, the fiber is completely aromatized. The cyclization leads to an imperfect packing of the chains, resulting in an intermediate increase of L and V_{rel} as well as a decrease of l_p. In the completely cyclized fiber, especially in the case of the copolymer fiber, the packing is more perfect, as indicated by the low values of V_{rel}. The aromatization leads again to a more imperfect packing due to the increased stiffness and the cross-linking of the chains. This results in a strong increase of V_{rel} and very low values of l_p. The formation of larger polycyclic aromatic units at higher temperatures does not, apparently, improve the packing, so that the microvoid structure at 470 °C is comparable to that of carbon fibers.

5 Conclusions

The results of the present study can be summarized as follows:

1. The microvoid structure and the microvoid content of heat-treated PAN fibers is correlated to the cyclization and the aromatization reaction (descibed in detail in a second paper)[9] in the sense that it shows the influence of chain structure and perfection on the molecular packing.

2. In the pristine fibers, the microvoid content is of the order of one volume percent. The length of the microvoids is 30−40 nm and the diameter 2−3 nm.

3. Partial cyclization (phase α) produces an increase of the microvoid content, an increase of the length, and a decrease of diameter.

4. In fully cyclized copolymer fibers, volume content and length and diameter of the microvoids are comparable to those of the pristine fibers. In homopolymer fibers, the fully cyclized state is somewhat different.

5. The aromatization leads to a microvoid content of the order of 10−20 volume percent, lengths of about 40 nm, and diameters of 0.5 nm. The latter value is comparable to those found in carbon fibers of low heat treatment temperature.

6. The method of evaluation developed for this study may be useful for the investigation of microvoids in other fibers.

Acknowledgment. We thank Dr. Fester (Hoechst AG) for the PAN fibers and Dr. R. Zietz for his assistance in connection with the SAXS measurements at DESY.

References and Notes

(1) Ruland, W. *J. Polym. Sci.* **1969**, *C28*, 143−151.
(2) Perret, R.; Ruland, W. *J. Appl. Crystallogr.* **1969**, *2*, 209−214.
(3) Perret, R.; Ruland, W. *J. Appl. Crystallogr.* **1970**, *3*, 525−532.
(4) Debye, P.; Anderson, H. R.; Brumberger, H. *J. Appl. Phys.* **1957**, *28*, 679−683.
(5) Dobb, M. G.; Johnson, D. J.; Saville, B. P. *J. Polym. Sci. Polym. Symp.* **1977**, *58*, 237−241.
(6) Northolt, M. G.; van Aartsen, J. J. *J. Polym. Sci. Polym. Symp.* **1977**, *58*, 283−287.
(7) Tillgner, H. Diploma Thesis, Marburg, 1986.
(8) Maskos, M. Diploma Thesis, Marburg 1992.
(9) Thünemann, A. F.; Ruland, W. *Macromolecules*, submitted for publication, 1999.
(10) Ruland, W. *Colloid Polym. Sci.* **1977**, *255*, 833−836.
(11) Ruland, W. *J. Appl. Crystallogr.* **1968**, *1*, 90−101.

MA991427X